International Journal of Pharmaceutics 415 (2011) 259–266

Contents lists available at ScienceDirect

International Journal of Pharmaceutics

journal homepage: www.elsevier.com/locate/ijpharm

Pharmaceutical Nanotechnology

Chitosan-modified poly(D,L-lactide-co-glycolide) nanospheres for plasmid DNA delivery and HBV gene-silencing

Ping Zeng[a], Yi Xu[b], Chunhua Zeng[a], Hong Ren[a], Mingli Peng[a,*]

[a] Key Laboratory of Molecular Biology of Infectious Disease, Chongqing University of Medical Science, Chongqing 400016, PR China
[b] Chemistry and Chemical Engineering College, Chongqing University, Chongqing 400030, PR China

ARTICLE INFO

Article history:
Received 5 March 2011
Received in revised form 26 April 2011
Accepted 20 May 2011
Available online 27 May 2011

Keywords:
Poly(D,L-lactide-co-glycolide)
Hepatitis B virus
Gene therapy
Chitosan
Nanoparticles

ABSTRACT

Gene silencing using small interfering RNA (siRNA) has several potential therapeutic applications. In the present study, we investigated nanoparticles (NS) formulated using the biodegradable polymer, poly(D,L-lactide-co-glycolide) (PLGA) for plasmid DNA (pDNA) delivery. A cationic polymer, Chitosan (CHS), was incorporated in the PLGA matrix to improve pDNA loading efficiency and cellular uptake ability. PLGA–CHS NS were prepared by a spontaneous emulsion diffusion (SED) method, and various formulation factors were investigated. Spherical nanoparticles with particle size of around 60 nm were obtained under optimum formulation condition. The effectiveness of pDNA-loaded PLGA–CHS nanoparticles in expressing the indicative enhanced Green Fluorescent Protein (eGFP) and in slicing Hepatitis B virus (HBV) gene were examined in HepG2.2.15 cells. CHS-modified PLGA NS exhibited much higher loading efficiency than unmodified PLGA NS. CHS–PLGA NS showed a positive zeta potential, while plain-PLGA NS were negatively charged. EGFP expression studies by observation with confocal leaser scanning microscopy (CLSM) indicated that pDNA-loaded CHS–PLGA NS were more effectively taken up by the cells than plain-PLGA NS. The corresponding results showed that the HBV gene-silencing efficiency of CHS–PLGA NS was higher than those of plain-PLGA NS and naked pDNA. Thus, CHS–PLGA NS containing pDNA could provide an effective pDNA delivery system in vitro, showing that such an approach could be useful in the treatment of viral diseases in vivo.

1. Introduction

Gene therapy is recognized as one of the most promising approaches for treatment of serious diseases, including monogenic diseases, infectious diseases and cancer (Verma and Somia, 1997). In this respect, Hepatitis B virus (HBV) is the most common infectious diseases, with a rising incidence worldwide, which substantially increases the risk of chronic liver disease and hepatocellular carcinoma in humans. RNA interference (RNAi) of virus-specific genes has emerged as a potential antiviral mechanism.

It is interesting to note that inhibiting the expression of HBV X region (HBV-X) is a potentially powerful therapeutic approach for treating HBV infectious diseases.

Exogenous gene expression in vitro and vivo for therapeutic purposes will require methods that allow for transferring gene into cells efficiently. In this respect, a variety of viral vectors have been used for introducing genes into the cells, including adeno-associated virus (Nakai et al., 1998), retroviruses (Kitten et al., 1997), and adenoviruses (Gerolami et al., 2004), but they are associated with immunogenicity, oncogenic properties and unknown long-term effects. On the other hand, many non-viral vectors have been reported that were gene gun (Yoshida et al., 1997), cationic lipids (Wiethoff et al., 2004), cationic polymers (Kim and Kim, 2009), electroporation (Suzuki et al., 1998) and others. However, some cationic compounds show cytotoxic effects and limited transfection efficiency. Therefore, the development of novel vector systems with improved targeting specificity, higher transfection efficiency and improved safety is necessary.

In recent years, significant effort has been put into developing nanotechnology for drug delivery, since it offers a suitable means of delivering small molecular weight drugs, as well as macromolecules such as proteins, peptides and genes, by either localized or targeted delivery to the tissue of interest (Moghimi et al., 2001). In particular, biodegradable nanospheres are available for delivering drugs and are degraded after passing a required specific site. Among these, poly(D,L-lac-tide-co-glycolide) (PLGA) has been approved by the FDA for certain human clinical uses such as resorbable sutures, bone implants and scaffolds in tissue engineering (Panyam and Labhasetwar, 2003; Hirosue et al., 2001;

* Corresponding author at: 76# Linjiang Road, The Institute of Viral Hepatitis, The Second Affiliated Hospital, Chongqing University of Medical Science, Chongqing 400010, PR China. Tel.: +86 23 63693225; fax: +86 23 63822696.
E-mail address: minglip55@yahoo.com.cn (M. Peng).

0378-5173/$ – see front matter © 2011 Elsevier B.V. All rights reserved.
doi:10.1016/j.ijpharm.2011.05.053

Perez et al., 2001). PLGA NS have also demonstrated potential for sustained nucleic acid (e.g. pDNA, antisense oligonucleotides, and siRNA) delivery (Khan et al., 2004). Previous studies have shown that PLGA NS are non-toxic and biocompatible (Panyam et al., 2003), and are suitable for gene delivery applications in vitro and in vivo (Perlstein et al., 2003).

Our studies indicate that nanoparticles fabricated using PLGA alone result in poor encapsulation of pDNA. We rationalized that introduction of Chitosan (CHS), a cationic polymer commonly used in gene delivery applications, in the PLGA matrix could improve the retention of anionic pDNA. In this experiment, we have investigated the usefulness of cationic charged CHS-modified PLGA NS to improve bioavailability and for a liver pDNA gene delivery system in hepatocellular cells. A number of liver diseases are the candidates for liver gene delivery. In particular, HBV has attracted particular attention as targets of siRNA therapy. The aims of this study are to evaluate pDNA-loaded PLGA NS for cellular uptake and RNAi effects using HepG2.2.15 cells in vitro.

2. Materials and methods

2.1. Materials

Poly(D,L-lactic-co-glycolic acid) (PLGA; lactic-glycolic acid ratio: 75:25, Mr = 40,000 and inherent viscosity 0.22 dl/g) was purchased from Aldrich–Sigma, Germany. Polyvinyl alcohol (PVA, average Mw 13–23:kDa, 87–89% hydrolysed) and Chitosan hydrochloride (83% deacetylated) were obtained from Sigma, UK. HepG2.2.15 human liver tumor cells were purchased from our lab. RPMI 1640 was purchased from Gibco (Basel, Switzerland). Lipofectamine™ 2000, Opti-MEM I reduced serum medium and fetal bovine serum (FBS) were purchased from Invitrogen, UK. 3-(4,5-Dimethyl-thiazol-2-yl)-2,5-diphenyl-tetrazolium bromide (MTT) was purchased from Sigma, UK. A coden-optimized plasmid DNA containing the eGFP and SiRNA which targeted against HBV-X gene (sense: 5′-ACCGTCTGTGCCTTCTCATCTTTT-3, antisense: 3′-TTTTGGCAGACACGGAAGAGTA-5′) were synthesized by corporation of Sangon (Shanghai, China). All other chemicals and reagents used in this study were analytical grade.

2.2. Preparation of PLGA–CHS NS with adsorbed pDNA

The preparation method of PLGA–CHS NS was a modification of the technique described by Kumar et al. (2004). Briefly, a solution of 5% (m/v) PLGA in dichloromethane and acetone was stirred for 30 min. This organic phase was poured into an aqueous phase with 5% (m/v) PVA solution in double distilled water under stirring, followed by ultrasonication (Soniprep, JY88-II, Ningbo, Chain) on ice for 4 min with 80% power output, pulse duty 0.5 s per cycle. The dichloromethane and acetone were evaporated before centrifuging (Hitachi Himac CR21F, Japan) at 20,000 rpm for 30 min twice by re-suspending the nanoparticles collected as a pellet in 50 mL distilled water. For the preparation of CHS-modified PLGA NS, chitosan (0.2% (w/v) in 0.5 M acetate buffer, pH 4.4)–PVA (5% (w/v) in distilled water) mixed solution was used as the dispersing phase for the emulsion solvent diffusion process. PVA is surfactant, therefore excess PVA (not adsorbed on the NS surface) should be removed by repeated centrifugation to avoid the adverse effect on cell growth.

pDNA adsorption onto PLGA–CHS NS was carried out in phosphate buffer pH 7.4. A fixed amount of pDNA was added drop-wise to an equal volume of various concentrations of PLGA–CHS NS depending on weight ratio of PLGA–CHS and pDNA. The suspension was then briefly mixed and incubated at room temperature for 1 h.

2.3. Photon correlation spectroscopy

Hydrodynamic diameter was determined by photon correlation spectroscopy (PCS) on Microtrac S3500 (Microtrac Inc., USA). For measurements of particle size, all samples were diluted 50 fold in demineralized water, resulting in comparable viscosities.

2.4. Zeta potential measurements

Zeta potential of nanoparticles was determined using zeta potential analyzer (Nano ZS90, Malvern Instruments, England). For the determination of zeta potential, samples were diluted with PBS to an appropriate concentration. To measure the zeta potential of the nanoparticles as a function of pH, both chitosan-coated and noncoated nanoparticles suspensions were diluted with PBS buffer of different pH values ranging from 3 to 10. The pH was adjusted to 2 by using HCl (1 N) before titration to pH 10 with NaOH (0.1 N). Measurements of the zeta-potential were carried out at 1.0 pH increments at 25 °C.

2.5. Transmission electron microscope

The morphology of the NPs was determined by transmission electron microscopy (TEM). For TEM, a drop of nanoparticles suspension was placed on to the TEM (Tecnai 20, Philips/FEI Inc., Netherlands with accelerating voltage of 200 kV) grid and dried in room temperature. Diameter of nanoparticles was measured from five to seven different TEM fields to determine the average particle size of nanoparticles.

2.6. Gel electrophoresis and determination of unbound pDNA

The binding of pDNA with PLGA–CHS NS was determined by 1% agarose gel electrophoresis using TAE buffer (242 g Tris, 57.1 mL glacial acetic acid, and 0.5 mM EDTA, pH ~8.0) containing 0.5 μg/mL ethidium bromide. PLGA–CHS–pDNA nanopaticles were loaded with series of different ratios (w/w) of pDNA to PLGA–CHS nanopaticles. A 1:6 dilution of loading dye was added to each well and electrophoresis was carried out at a constant voltage of 80 V for 34 min. The pDNA bands were then visualized under a UV transilluminator at a wavelength of 365 nm.

2.7. Cytotoxicity assay

Cytotoxicity of nanoparticles was determined using MTT assay in HepG2.2.15 cells. The general cytotoxicity test followed the method of Katas et al. (2009) HepG2.2.15 cells were seeded in a 96-well plate at a density of 4000 cells per well in RTMI 1640 medium containing 10% of FBS and grown overnight. After 48 h incubation of PLGA–CHS–pDNA NS, PLGA–CHS NS or Lipofectamine™ 2000 at 37 °C, 20 μL of MTT (3-(4,5-dimethyl-thiazol-2-yl)-2,5-diphenyl tetrazoliumbromide, 5 mg/mL (m/v)) in sterile PBS was added to each well and then incubated for 4 h to allow formation of formazan crystals. After this, the unreduced MTT and medium was removed and the cells were washed with PBS. 200 μl of DMSO was then added to each well to dissolve the MTT formazan crystals and the plate was incubated at 37°C for 5 min. The absorbance of formazan products was measured at 490 nm using a microplate reader (LMAX II384, Molecular Device Inc., USA).

2.8. Biological activity of PLGA–CHS–pDNA NS

In vitro transfection studies were performed in HepG2.2.15 cells. The cells were seeded in a 6-well plate at a density of 3×10^5 cells per well in RPMI 1640 containing 10% of FBS without antibiotic, 24 h prior to transfection. The following day, medium was

removed and PLGA–CHS–pDNA NS, PLGA–pDNA NS, PLGA–CHS NS or Lipofectamine™ 2000–pDNA (Lip–pDNA) that were diluted with Opti-MEM were then added to the cells and incubated at 37 °C with a 5%CO2 atmosphere for 6 h. Following 6 h of transfection period, the medium was removed and the cells were washed with PBS twice, after this, media was replaced with 2 mL fresh medium containing serum. After 72 h, the signal of eGFP was determined using confocal laser microscopic Assay System (LEICA TCS SP2, Leica Instruments, Germany). As controls, 2 μg plasmid DNA were also included in bioactivity evaluation.

2.9. Silencing HBV gene

HepG2.2.15 cells were treated with PLGA–pDNA, PLGA–CHS–pDNA and Lip–pDNA for 72 h, both adherent and floating cells were collected, and then PT-PCR and Western blot analysis were performed. For Western blot, protein concentration was determined using the BCA Protein Assay kit (Pierce Chemical, USA). Thirty micrograms of total proteins was subjected to 10% SDS-PAGE and electroblotted onto a PVDF membrane (Millipore Corporation, USA). After blocking, membranes were incubated anti-HBcAg (1:2000 dilution, Abcam, USA) and anti-HBsAg (1:2000 dilution, Abcam, USA) and secondary antibodies conjugated with horseradish peroxidase (1:3000 dilution, Abcam, USA). β-Actin antibody (1:2000 dilution, Abcam, USA) was probed as an internal control. Protein bands were visualized by using CN/DAB Substrate Kit (Pierce Chemical). The bands were analyzed with Quantity One-4.6.2 Basic software (Bio-Rad, USA).

Total RNAs were isolated from culture cells (1×10^6) transfected with PLGA–pDNA, PLGA–CHS–pDNA and lip–pDNA for 72 h. RNA concentrations and purity were determined by measuring the absorbance A260 nm/A280 nm ratio. cDNA was then prepared from the RNA samples and real time PCR was carried out using SYBR® PrimeScript® RT-PCR Kit (Takala, Japan) according to the manufacturer's instructions .Amplification was performed on a real-time thermocycler (ABI7300 system, USA). Melting curves and agarose gel electrophoresis were used to control the specificity of the PCR. Gene expression was analyzed using the following pairs of primers: HBV-X (forward, 5′-CGTCCTTTGTTTACGTCCCG-3′; reverse, 5′-GAGAGGTGCGCCCCGTGGTCG-3′), HBV-S (forward, 5′-GTTGACAAGAATCCTCACAATACCG-3′; reverse, 5′-ACATCCAGCGTAAACCAGGACAAGT-3′), β-actin (forward, 5′-CCCAGGCACCAGGGCGTGATGGT-3′; reverse, 5′-GGACTCCATGCCCAGGAAGGAA-3′). PCR results were then normalized to the levels of β-actin and calculated by reference to the average value for the control group using the comparative Ct method. For each sample and each gene, PCR reactions were carried out in triplicate and repeated three times.

3. Results and discussion

3.1. Particle size

Various formulation factors and physicochemical properties of the nanoparticles play key roles in biological applications. The particle size is considered one of the most important parameters in the mucosal, tissue and cell uptake of the nanoparticles (Tahara et al., 2009). Smaller nanoparticles are able to penetrate through the submucosal layers, whereas larger size particles were found to be localized in the epithelial lining (Song et al., 1998). Moreover, smaller nanoparticles were found to show significantly higher transfection efficiency as compared with larger nanoparticles (Prabha et al., 2002). Therefore, our study aimed to produce nanoparticles of relatively smaller size while being able to adjust different formulation factors deliberately.

3.1.1. Effect of acetone to dichloromethane volume ratio

In the preparation process, CHS coated PLGA NS were prepared using the SED method. PLGA was dissolved in acetone and dichloromethane with the corresponding properties of

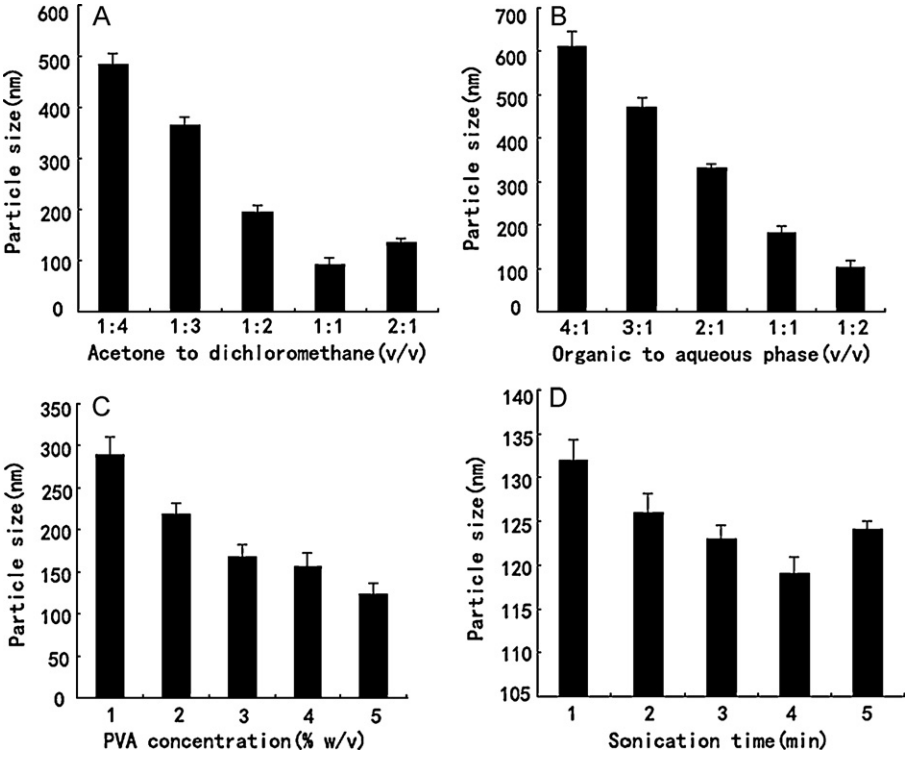

Fig. 1. Effect of the formulation parameter on the particle size of chitosan-coated PLGA nanoparticles. (A) Acetone to dichloromethane volume ration, (B) organic to aqueous phase volume ratio, (C) the concentration of PVA and (D) sonication time. Each bars represents the mean ± SD ($n = 3$).

hydrophilicity and hydrophobicity. Due to the use of acetone in this method, particle formation was observed immediately after mixing the organic and aqueous phases since acetone is highly miscible with water and could rapidly diffuse into the aqueous phase. The morphology and size of nanoparticles were also influenced by the amount of acetone added to the PLGA. Therefore, the amount of acetone added was specified as acetone to dichloromethane volume ratio, ranging from 1:4 to 2:1. Increasing the amount of acetone in comparison to dichloromethane resulted in the reduction of particle size. When the volume ratio was increased to 1:1, the mean particle diameter was significantly reduced to 93 ± 13 nm (Fig. 1A), whereas further increase in the volume ratio led to little increase in the particle size (Fig. 1A).

3.1.2. Effect of organic to aqueous phase volume ratio

The ratio between the organic and aqueous phase of the emulsion is of great importance regarding the stability of the emulsion and is expected to influence the size of the dispersed globules. Therefore, the organic to aqueous phase volume ratio was varied among 4:1, 3:1, 2:1, 1:1, and 1:2. The results demonstrate a gradual decrease in particle size by changing the ratio from 4:1 to 1:2 (Fig. 1B). When the volume ratio was increased to 1:2, the mean particle diameter was significantly reduced to 102 ± 15 nm (Fig. 1B). The significant decrease in particle size may be due to the increased aqueous phase. Under the lower ratio between aqueous and organic phase, organic solution was difficult to diffuse into the aqueous phase which resistance to the shear forces and hinder the nanoparticle formation. Moreover, the concentration of nanoparticles was very high so that nanoparticles can easily aggregate.

3.1.3. Effect of concentration of surfactant and sonication time

The influence of sonication time on the colloidal properties of the chitosan-coated PLGA NS was studied. Different sonication times were used in the preparation of PLGA–CHS NS which were 1-5 min. An increase in sonication time resulted in a corresponding decrease in the particle size (Fig. 1D); however, no significant reduction in size was observed by increasing the time above 4 min. Further increase in the sonication time was not favorable, because the high energy provided led to particle fusion and aggregation rather than particle size reduction.

In addition to the sonication time, the PVA content is also considered one of the most important parameters which strongly influenced the particle size. Five different concentrations were used in the preparation of PLGA–CHS NS which were 1, 2, 3, 4 and 5% (m/v). In general, it was observed that increasing the concentration of PVA from 1% to 5% (m/v) resulted in a statistically significant decrease in the mean particle size (Fig. 1C). Therefore, the amount of surfactant plays an important role as a stabilizing agent in the emulsification process and in the protection of the droplets. Increasing the concentration of PVA in the aqueous phase resulted in a corresponding increase in the viscosity. This contributes in the formation of a stable emulsion with smaller and uniform droplet size, leading to the formation of smaller sized nanoparticles (Sanjeeb et al., 2002). Whereas, the more PVA will induce more residual PVA and nanoparticles with higher amount of residual PVA had relatively lower cellular uptake despite their smaller particle size (Sanjeeb et al., 2002). So, appropriate concentration of PVA is an important formulation parameter. At last, as shown in Fig. 2A and B, significant differences in particles size distribution between before and after optimization were measured by PCS. After optimization, the average size was 59.43 ± 14 nm which was approved by the TEM images (Fig. 2C). These results appear that the nanospheres were uniform and spherical in shape with smooth surfaces when optimum formulation parameter were used in the preparation process.

3.2. Zeta potential of nanoparticles

In addition to the particle size of the nanoparticles, the zeta potential of nanoparticles is also considered one of the most important parameters in the cellular uptake ability and particle stability.

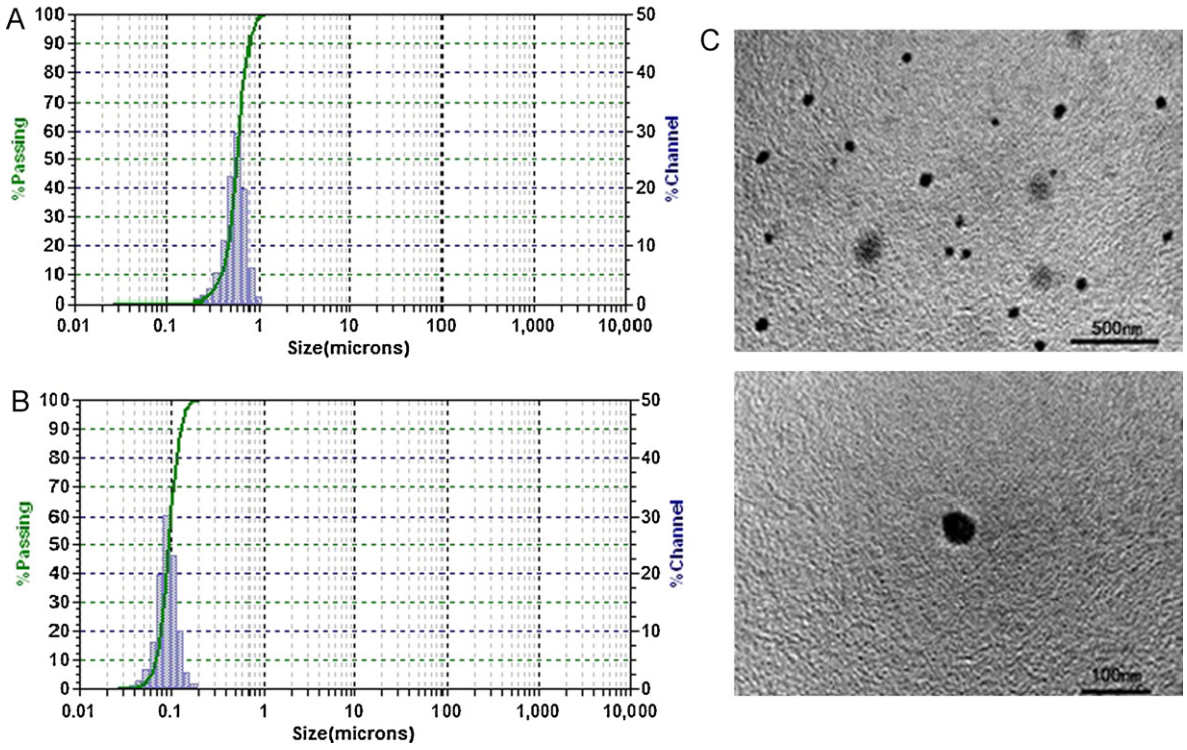

Fig. 2. Particle size distributions and surface morphology of the PLGA–CHS NS were measured by PCS and TEM. (A) Before optimization, (B) after optimization and (C) TEM images of chitosan-coated PLGA nanoparticles after optimization.

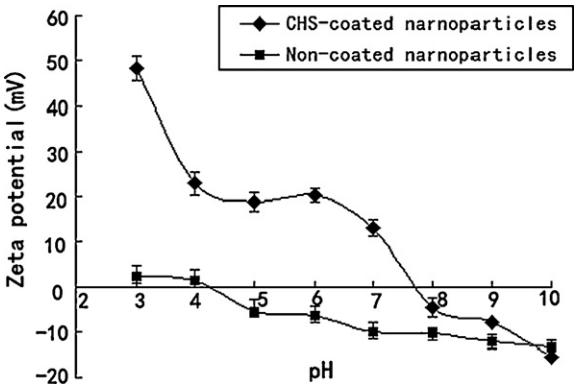

Fig. 3. Zeta potential–pH profile for noncoated and chitosan-coated PLGA nanoparticles. Each bar represents the mean ± SD for $n = 3$.

In theory, the electrostatic repulsion between particles with the same electric charge prevents the aggregation of the nanoparticles (Kumar et al., 2004). Moreover, more pronounced positive charge on the surface of nanoparticles will facilitate their adherence to the negatively charged cellular membranes and consequently increase their intracellular uptake, which was demonstrated by transfection experiments. In this paper, the presence of chitosan increased the zeta potential of nanoparticles to 13.2 mV compared with −10 mV for the plain PLGA NS in PBS (pH 7.8), as shown in Fig. 3. The zeta potential shifted to positive values due to the CHS adsorbed on the surface of PLGA NS. Chitosan is a weak base polysaccharide, consisting of β-(1,4) linked monomers of D-glucosamine and N-acetyl-D-gluco-samine. The PLGA molecular structure could efficiently interact with CHS amino groups once they were ionized in aqueous medium. Consequently, the protonation of the amino group of CHS results in positive zeta potential. On the contrary, the dissociation of the carboxyl group of PLGA results in negative zeta potential.

At the same time, the effect of pH on the surface charge of chitosan-coated and noncoated PLGA NS was investigated. As shown in Fig. 3, the zeta potential of the plain PLGA NS is constant (−12.3 to 2.3 mV) at all pH values tested. In comparison, CHS-coated PLGA NS showed an increasing potential along with the decreasing pH values, especially 50 mV in pH 3. The phenomenon reveals that the surface charge of nanoparticles is strongly dependent on pH. Thus, the zeta potential provided proof of successful cationic surface modification by the addition of chitosan.

3.3. pDNA loading efficiency

Although the improvement of the colloidal characteristics of the nanoparticles was an essential part, the ability of these nanoparticles to bind pDNA also required investigation. Analysis of pDNA loading efficiency adsorbed onto the PLGA–CHS NS with sizes around 100 nm was performed using the highest concentration of PVA (5% (m/v), 13–23 kDa) and pDNA was adsorbed onto the particles (in phosphate buffer, 0.2 M, pH 7) at different ratios (w/w) of PLGA–CHS NS to pDNA, ranging from 50:1 to 100:1. The pDNA loading efficiency was studied using analysis of the electrophoretic mobility of the pDNA within 1% agarose gel and the results showed a significantly increased pDNA loading efficiency along with the ratio (w/w) from 25:1 to 100:1. Especially, nearly 100% of pDNA loading efficiency was achieved at the ratio of 100:1 and at this point, pDNA was completely bound to the PLGA–CHS NS (Fig. 4).

In contrast to that, studies have shown that PLGA alone was unable to adsorb pDNA even though equivalent amount to the PLGA–CHS NS at ratio of 100:1 were used in which the ratio could attribute to the complete binding of pDNA onto the surface of PLGA–CHS NS (Fig. 4). The phenomenon may be due to the electrostatic binding of the negatively charged pDNA to the positively charged nanoparticles rather than plain PLGA NS.

3.4. Cytotoxicity of PLGA–CHS NS

The cytotoxicity effects of PLGA -CHS NS as a delivery system for pDNA to the cells was investigated in HepG2.2.15 cell lines, using MTT assays. The results obtained revealed that loss of cell viability in HepG2.2.15 cells appeared to be sensitive to the amount of PLGA–CHS–pDNA NS (Fig. 5). Consequently, cell cytotoxicity was evaluated in the dose range that was used in the gene silencing studies. In HepG2.2.15 cells, the loss of cell viability was increased with the increasing amount of PLGA–CHS–pDNA NS (Fig. 5). Approximately 25% loss of cell viability was observed at 24 h post-incubation for 5 mg/mL PLGA–CHS NS compared to less than 10% cell loss at 1 mg/mL. However, the effect was transient as the cell viability was less affected at 48 h post-incubation. The percentage of cell viability in HepG2.2.15 cells was increased at 48 h post-incubation, in comparison with 24 h, for the cells incubated with PLGA–CHS–pDNA NS and Lipofectamine™ 2000–pDNA (Lip–pDNA). This illustrated that the particles had little adverse effect on cell growth.

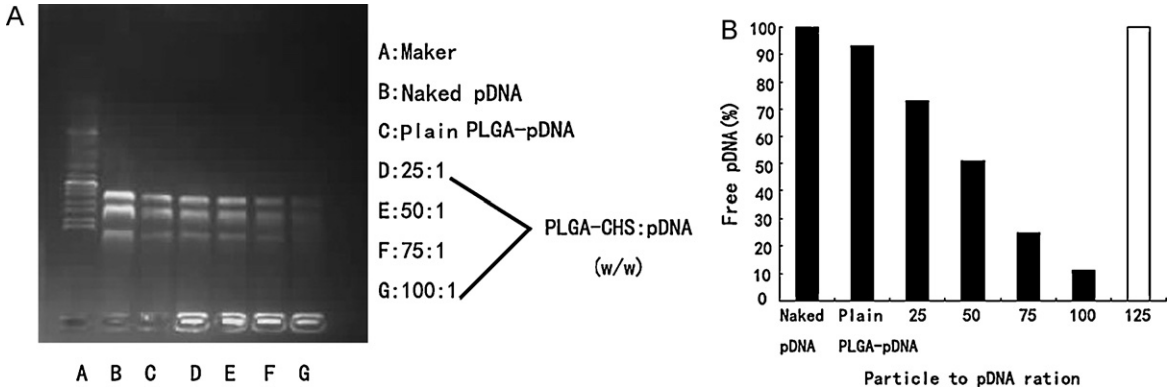

Fig. 4. PLGA–CHS nanoparticles binding efficiency and loading capacity to adsorb pDNA. (A) PLGA–CHS–pDNA complexes with increasing amounts of PLGA–CHS NS were prepared and analyzed for pDNA immobilization ability. Electrophoresis was carried out using 1% agarose gel in TAE buffer containing 0.5 μg/mL ethidium bromide at pH 8. (B) The amounts of free DNA were related to naked pDNA (100% mobile) run on the same gel. To quantify the pDNA-immobilization ability, the PLGA–CHS NS: pDNA ratios (w/w) required for 100% immobilization are compared in this graph (solid bars = Percentage of free DNA; white bars = 100% immobilization).

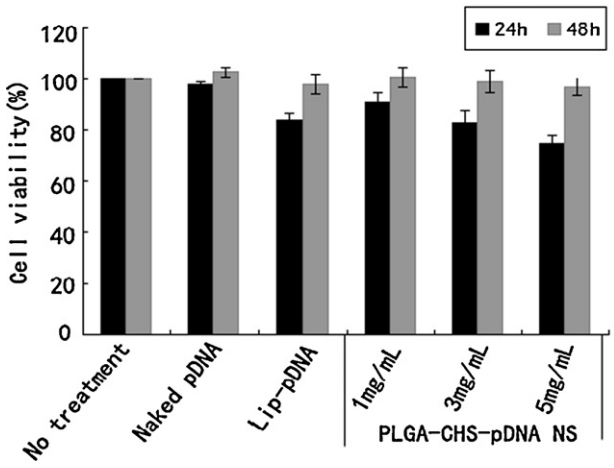

Fig. 5. Toxicity effect of PLGA–CHS nanoparticles with adsorbed pDNA in HepG2.2.15 cells at 5×10^3/well (each bar represents the mean ± SD ($n = 3$).

3.5. Transfection studies of PLGA–CHS with adsorbed pDNA

Biological activity studies of pDNA adsorbed onto PLGA–CHS NS were assessed in HepG2.2.15 cell lines. In this study, only particles with a particle size around 100 nm were used with 100:1 weight ratio of PLGA–CHS to pDNA. The eGFP signal increase was closely correlated with successful transfection of pDNA as well as expressing of pDNA. We demonstrated that eGFP expression intensity could be used as an indicator of transfection efficiency. Normal HepG2.2.15 cells showed no distinct eGFP fluorescence. The eGFP fluorescence intensity of the different PLGA–CHS–pDNA NS, plain PLGA–pDNA NS, PLGA–CHS NS, naked pDNA and Lip–pDNA were evaluated visually using confocal laser scanning microscopy (CLSM), as shown in Figs. 6 and 7.

After naked pDNA was transfected into the HepG2.2.15 cells, eGFP fluorescence was not observed in the cells, as shown in Fig. 6A. This was because pDNA is a hydrophilic polymer, and the strong negative charge derived from phosphate group makes it very difficult for penetration of naked pDNA into cell without a transfecting

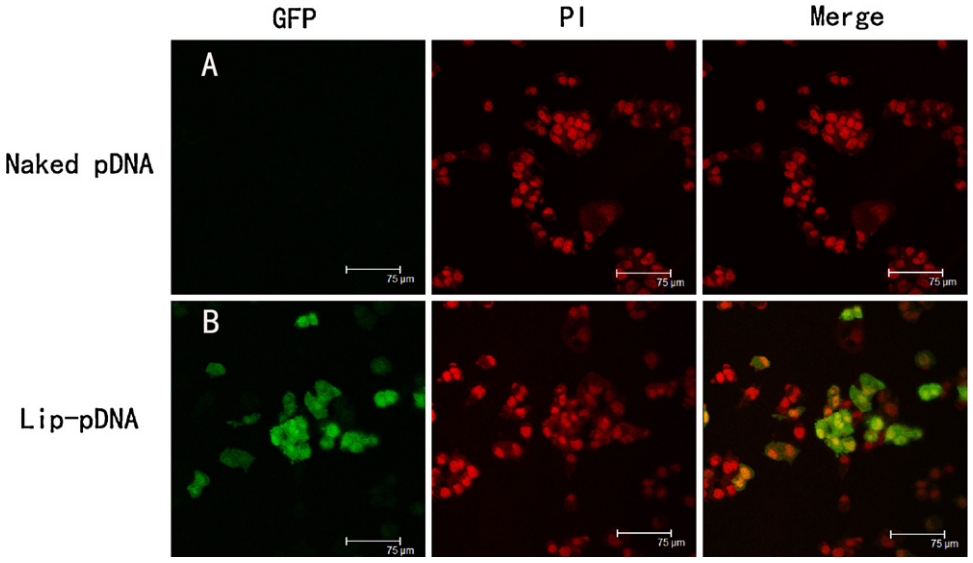

Fig. 6. Confocal laser microscopic images of HepG2.2.15 cells following 48 h transfection with (A) naked pDNA and (B) Lip–pDNA complexes were used to treat HepG2.2.15 cells. Scale bar = 75 μm.

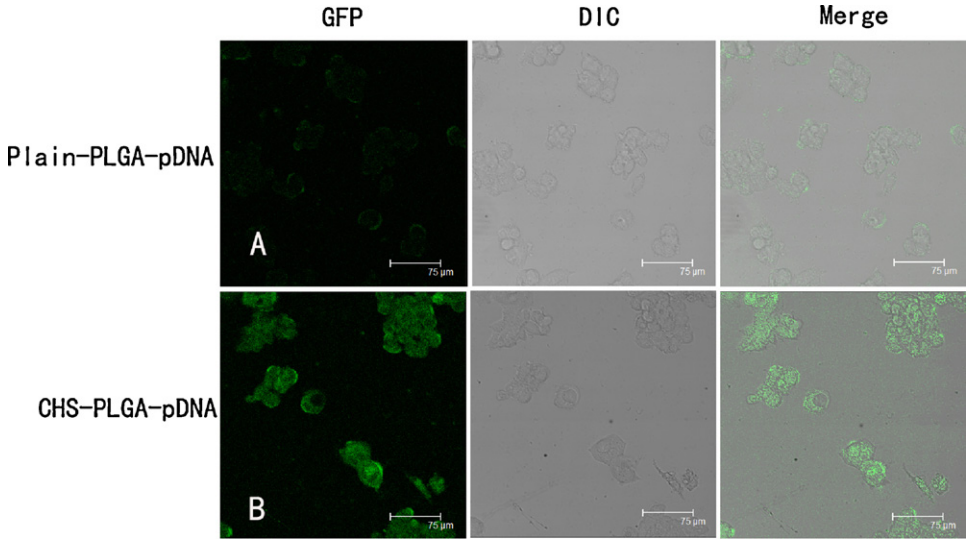

Fig. 7. Confocal laser microscopic images of HepG2.2.15 cells following 48 h transfection with (A) plain-PLGA–pDNA NS and (B) CHS–PLGA–pDNA NS were used to treat HepG2.2.15 cells. Scale bar = 75 μm.

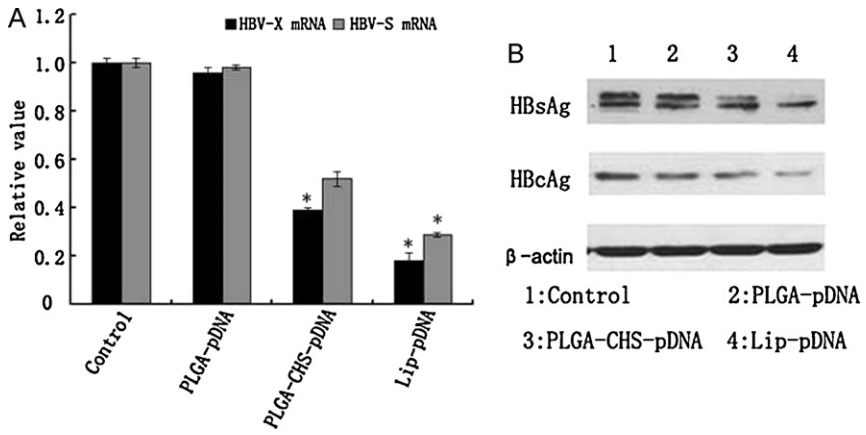

Fig. 8. HBV-X-siRNA reduces expression of HBV-X and HBV-S gene in HepG2.2.15 cells. The cells were treated with different transfection reagents for 48 h and the expression levels of targeted gene were examined by the real-time PCR and Western bolt. (A) HBV-X mRNA and HBV-S mRNA expression in the cells was determined by RT-PCR, untreated cells as a control. β-Actin was used as a loading control. (B) Protein expression in the cells was determined by Western bolt, untreated cells as a control. β-Actin was used as a loading control. Each bars represents the mean ± SD ($n = 3$) (*$p < 0.1$, significantly different compared with control).

reagent (Tahara et al., 2010). GFP fluorescence could be observed in the cells that were PI-dyed using Lipofectamine™ 2000 as a transfecting reagent (Fig. 6B). The green fluorescence of eGFP in the images was changed to a yellow color to provide a better illustration of the localization of eGFP. We found that eGFP expressed not only in the cytosol but also in the nucleus. The eGFP expression intensity was very high, that because Lipofectamine™ 2000 is a cationic lipid that can easily form electrostatic complexes with pDNA and pDNA/cationic lipid complexes were easily transfected.

The eGFP expression intensity in HepG2.2.15 cells also showed a higher intensity after transfection with PLGA–CHS–pDNA NS (200 μg/2 μg) complexes compared with equal amount of plain PLGA–pDNA NS, as shown in Fig. 7. The result might have been caused by the higher cellular uptake ability of CHS-modified PLGA NS. The zeta potential of CHS-modified PLGA NS proved to be strongly positive charged. These results suggested that cationic CHS on the surface of nanoparticles enhanced the association between CHS-modified PLGA NS and negatively charged cell membranes by electrostatic interactions and that nanoparticles cellular uptake might be increased. Furthermore, the pDNA loading efficiency of plain PLGA NS was lower compared with CHS-modified PLGA NS, as shown in Fig. 4.

On the other hand, the blank PLGA NS, used as a positive control, showed an interesting phenomenon. We found that blank PLGA nanoparticle treated cells showed autofluorescence (not shown), but the intensity was very weak compared with PLGA–CHS–pDNA treated cells. Unfortunately, the reasons cannot be explained clearly.

3.6. Effects of chitosan modification on the gene-silencing effect

The primary measure of HBV-X-siRNA-mediated effects is the silencing of the target mRNA, which should result in the corresponding reduction of HBcAg and HBsAg. To test the silencing efficiency of HBV-X mRNA and HBV-S mRNA, we have used the RT-PCR method to determine target mRNA in HepG2.2.15 cell. As shown in Fig. 8A, in the HepG2.2.15 cells transfected with PLGA–CHS–pDNA for 72 h, the levels of the HBV-X mRNA and HBV-S mRNA were noticeably reduced to 0.39 ± 0.02-fold and 0.49 ± 0.01-fold compared with control. The HBV-X gene-silencing efficiency of CHS-modified PLGA NS was higher than PLGA–pDNA and control, but showed a lower gene-silencing efficiency compared with Lipofectamine™ 2000.

Furthermore, western blotting was used to examine the effects of HBV-X-siRNA treatment on the levels of protein. As shown in Fig. 8B, the transfection of HBV-X-siRNA directed against HBV-X-mRNA resulted in significant decrease in protein levels after 72 h. In the HepG2.2.15 cells transfected with PLGA–CHS–pDNA and Lip–pDNA, the expression of HBcAg were decreased to 52% and 34% compared with control, the levels of HBsAg still were decreased to 62% and 41% compared with the control. The results indicated that in the group of PLGA–CHS–pDNA, the expressing of HBcAg and HBsAg were markedly down-regulated compared with PLGA–pDNA and control, but showed a lower decrease compared with Lipofectamine™ 2000.

Though Lip–pDNA complex have higher gene-silencing effect, some of the transfection reagents available commercially may have cytotoxicity and cannot be used in vivo. PLGA have been approved by the USA Food and Drug Administration (FDA) for limited clinical use. Chitosan as a surface modifier enhances the transport of nanoparticles into the cells and is biocompatible and biodegradable (Tahara et al., 2009). We previously found that CHS-modified PLGA NS did not show any cytotoxic effects for HepG2.2.15 cells, in contrast to Lip–pDNA complexes.

These results provide evidence that CHS-modified PLGA NS can be applied to the therapeutics for various diseases using pDNA, such as HBV infection. It is possible that PLGA–CHS NS might be developed as a non-viral vector for pDNA delivery in vivo due to a lack of side effects. Further studies concerning the transfection efficiency, HBV gene interfering effects in vivo, as well as the targeted pDNA delivery are currently underway.

4. Conclusions

PLGA nanoparticles for a liver gene delivery were prepared, and the activity in vitro was evaluated. Modification of PLGA NS by incorporating CHS as well as optimization of their preparation process has led to the formation of a better delivery system for pDNA with a higher transfection efficiency compared to pain PLGA. These non-viral vectors will be further evaluated for their in vivo abilities to provide pDNA carriers for the purposes of gene therapy in the field of liver disease.

Acknowledgements

The pDNA was generously provided by Dr. Tong-Chuan He (Molecular Oncology Laboratory, Department of Surgery, the University of Chicago Medical Center). This work was supported by the National Natural Science Foundation of China (30771921) (NSFC).

References

Gerolami, R., Uch, R., Faivre, J., Garcia, S., Hardwigsen, J., 2004. Herpes simplex virus thymidine kinase-mediated suicide gene therapy for hepatocellular carcinoma using HIV-1-derived lentiviral vectors. J. Hepatol. 40, 291–297.

Hirosue, S., Muller, B.G., Mulligan, R.C., Langer, R., 2001. Plasmid DNA encapsulation and release from solvent diffusion nanospheres. J. Control. Release 70, 231–242.

Katas, H., Cevher, E., Alpar, H.O., 2009. Preparation of polyethyleneimine incorporated poly(D,L-lactide-co-glycolide) nanoparticles by spontaneous emulsion diffusion method for small interfering RNA delivery. Int. J. Pharm. 369, 144–154.

Khan, A., Benboubetra, M., Sayyed, P.Z., Fox, S., Beck, G., Benter, I.F., 2004. Sustained polymeric delivery of gene silencing antisense ODNs, siRNA, DNAzymes and ribozymes: in vitro and in vivo studies. J. Drug Target 12, 393–404.

Kim, W.J., Kim, S.W., 2009. Efficient siRNA delivery with non-viral polymeric vehicles. Pharm. Res. 26, 657–666.

Kitten, O., Cosset, F.L., Ferry, N., 1997. Highly efficient retrovirus-mediated gene transfer into rat hepatocytes in vivo. Hum. Gene Ther. 40, 1491–1494.

Kumar, R., Bakowsky, U., Lehr, C.M., 2004. Preparation and characterization of cationic PLGA nanospheres as DNA carriers. Biomaterials 25, 1771–1777.

Moghimi, S.M., Hunter, A.C., Murray, J.C., 2001. Long-circulating and target specific nanoparticles: theory to practice. Pharmacol. Rev. 53, 283–318.

Nakai, H., Roland, W., Herzog, J., Hagstrom, N., 1998. Adeno-associated viral vector-mediated gene transfer of human blood coagulation factor IX into mouse liver. Blood 91, 4600–4607.

Panyam, J., Labhasetwar, V., 2003. Biodegradable nanoparticles for drug and gene delivery to cells and tissue. Adv. Drug Deliv. Rev. 55, 329–347.

Panyam, J., Dali, M.M., Sahoo, S.K., Chakravarthi, S.S., Amidon, G.L., Levy, R.J., Labhasetwar, V., 2003. Polymer degradation and in vitro release of amodel protein from poly(D,L-lactide-co-glycolide) nano- and microparticles. J. Control. Release 92, 173–187.

Perez, C., Sanchez, A., Putnam, D., Ting, D., Langer, R., Alonso, M.J., 2001. Poly(lactic acid)-poly(ethylene glycol) nanoparticles as new carriers for the delivery of plasmid DNA. J. Control. Release 75, 211–224.

Perlstein, I., Connolly, J.M., Cui, X., Song, C., Li, Q., Jones, P.L., Lu, Z., DeFelice, S., Klugherz, B., Wilensky, R., Levy, R.J., 2003. DNA delivery from an intravascular stent with a denatured collagen-polylactic-polyglycolic acid-controlled release coating: mechanisms of enhanced transfection. Gene Ther. 10, 1420–1428.

Prabha, S., Zhou, W.-Z., Panyam, J., Labhasetwar, V., 2002. Size-dependency of nanoparticle-mediated gene transfection: studies with fractionated nanoparticles. Int. J. Pharm. 244, 105–115.

Sanjeeb, K., Jayanth, P., Swayam, P., Vinod, L., 2002. Residual polyvinyl alcohol associated with poly(D,L-lactide-co-glycolide) nanoparticles affects their physical properties and cellular uptake. J. Control. Release 82, 105–114.

Song, C., Labhasetwar, V., Cui, X., Underwood, T., Levy, R.J., 1998. Arterial uptake of biodegradable nanoparticles for intravascular local drug delivery: results with an acute dog model. J. Control. Release 54, 201–211.

Suzuki, T., Shin, B.C., Fujikura, K., Matsuzaki, T., Takata, K., 1998. Direct gene transfer into rat liver cells by in vivo electroporation. FEBS Lett. 425, 436–440.

Tahara, K., Sakai, T., Yamamoto, H., Takeuchi, H., Hirashima, N., Kawashima, Y., 2009. Improved cellular uptake of chitosan-modified PLGA nanospheres by A549 cells. Int. J. Pharm. 382, 198–204.

Tahara, K., Yamamoto, K., Hirashima, N., Kawashima, Y., 2010. Chitosan-modified poly(D,L-lactide-co-glycolide) nanospheres for improving siRNA delivery and gene-silencing effects. Eur. J. Pharm. Biopharm. 74, 421–426.

Verma, I.M., Somia, N., 1997. Gene therapy: promises, problems and prospects. Nature 389, 239–242.

Wiethoff, C.M., Koe, J.G., Koe, G.S., Middaugh, C.R., 2004. Compositional effects of cationic lipid/DNA delivery systems on transgene expression in cell culture. J. Pharm. Sci. 93, 108–123.

Yoshida, Y., Kobayashi, E., Endo, H., Hamamoto, T., 1997. Introduction of DNA into rat liver with a hand-held gene gun: distribution of the expressed enzyme, [^{32}P]DNA, and Ca^{2+} flux. Biochem. Biophys. Res. Commun. 234, 695–700.